UCLA
UCLA Previously Published Works

Title

Metallic and Magnetic 2D Materials Containing Planar Tetracoordinated C and N

Permalink

Authors

Jimenez-Izal, Elisa
Saeys, Mark
Alexandrova, Anastassia N

Publication Date

DOI

Peer reviewed

Metallic and Magnetic 2D Materials Containing Planar Tetracoordinated C and N

Published as part of The Journal of Physical Chemistry virtual special issue "Mark S. Gordon Festschrift".

Elisa Jimenez-Izal,[†,‡] Mark Saeys,[§] and Anastassia N. Alexandrova*[,†,‖]

[†]Department of Chemistry and Biochemistry, University of California—Los Angeles, 607 Charles E. Young Drive, Los Angeles, California 90095-1569, United States

[‡]Kimika Fakultatea, Euskal Herriko Unibertsitatea (UPV/EHU), and Donostia International Physics Center (DIPC), P. K. 1072, 20080 Donostia, Euskadi, Spain

[§]Laboratory for Chemical Technology Gent, University Technologiepark, Zwijnaarde 914, 9052 Gent, Belgium

[‖]California NanoSystems Institute, Los Angeles, California 90095-1569, United States

Ⓢ *Supporting Information*

ABSTRACT: The top monolayers of surface carbides and nitrides of Co and Ni are predicted to yield new stable 2D materials upon exfoliation. These 2D phases are p4g clock reconstructed, and contain planar tetracoordinated C or N. The stability of these flat carbides and nitrides is high, and ab initio molecular dynamics at a simulation temperature of 1800 K suggest that the materials are thermally stable at elevated temperatures. The materials owe their stability to local triple aromaticity (π-radical, σ-radical, and σ-peripheral) associated with binding of the main group element to the metal. All predicted 2D phases are conductors, and the two alloys of Co are also ferromagnetic, a property especially rare among 2D materials. The preparation of 2D carbides and nitrides is envisioned to be done through surface deposition and peeling, possibly on a metal with a larger lattice constant for reduced affinity.
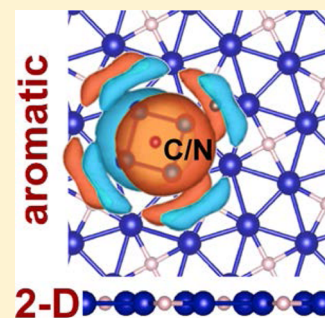
I. INTRODUCTION

Usually tetracoordinated carbon has a tetrahedral spatial arrangement due to its sp^3 hybridization. However, Hoffmann et al.[1] suggested that planar tetracoordinated carbon (ptC) could be stabilized (i) electronically, by using strong σ-donors or π-acceptors, (ii) mechanically, by constraining the ptC into a rigid steric framework, or (iii) by a combination of the two. Since then, several molecules containing this atypical ptC have been predicted and synthesized.[2−10] Planar tetracoordinated nitrogen, ptN, also has been predicted in NAl$_4^-$ and NSiAl,[8] and then in M$_n$N (M = BH, B, Al, Ga, In; n = 4, 5) and NAl$_3$X (X = N, P, As).[11−14]

The main focus of the design and rationalization of ptC and ptN has been on gas phase species, whereas the technological interest in materials is likely to be higher, because they can be more stable, made in larger quantities, and have interesting macroscopic properties. In this vein, a 2D TiC monolayer with quasi-planar ptC was predicted to have kinetic stability and anisotropic electronic properties.[15] Dai et al. searched for the most stable 2D Al$_x$C (x = 1/3, 1, 2, and 3) monolayers containing ptC,[16] among which AlC and Al$_2$C were found to be semiconductors, and Al$_3$C had a bandgap of 1.05 eV. A ptC-containing B$_2$C graphene structure was proposed[17] and predicted to be the first pristine 2D superconductor with a T_c higher than the boiling point of liquid helium.[18] Later, 2D penta-graphene was found,[19] where ptCs form pentagons, similar to the Cairo tiling. This new C allotrope can withstand

T up to 1000 K and has a quasi-direct band gap of 3.25 eV. Inspired by this finding, penta-B$_2$C was designed, consisting of pentagons containing two ptCs and a three-coordinated B.[20] It has a wide indirect band gap of 2.28 eV, and according to the DFT calculations, it can be switched to a metallic semiconductor under certain biaxial strains. Pancharatna et al. proposed a number of hypothetical extended networks containing ptC constructed from the C$_5^{2-}$ unit.[21] In addition, Wang et al. have recently reported the design of a Be$_5$C$_2$ monolayer on the basis of density functional theory calculations. This new 2D material contains quasi-planar pentacoordinated C and it is predicted to be stable, with moderate cohesive energy, positive phonon modes and high melting point, and delocalized bonding.[22] For periodic systems with ptN, Be-decorated BN, or BC$_2$N nanoribbons,[23,24] in which ptC and ptN coexist, were also predicted.

Upon exposure to hydrocarbons under catalytic conditions, ptC also forms on metal surfaces: on Co,[25−29] on Ni(100),[30,31] and on stepped Ni(111).[32,33] There, ptC plays a major role in defining surface morphology and as an initiation site for coking in catalysis. Surface carbides of Co and Ni show a p4g reconstruction, namely, a rotation of the two neighbor squares, along with a small expansion of the metal−metal distance, as

shown in Figure 1. They are extremely stable, competing with graphite on these metals, and with stability driven by the local aromaticity.[34] On the basis of this bonding principle, we further proposed that analogous aromatic p4g carbides should also form on the surfaces on Rh and Pd, and p4g nitrides should form on Co, Ni, and Rh.[34]

This previous work showed that the bonding effects leading to special stability are largely confined to the top monolayer in the surface alloys. Subsurface layers retain the geometric and electronic structures of the bulk metals. Intrigued by these observations, we now probe if the top monolayers forming on metal surfaces can be stable 2D materials.

II. COMPUTATIONAL METHODS

Plane-wave PAW-DFT calculations were done using VASP,[35−37] with GGA rPBE,[38,39] and an empirical dispersion correction (D2).[40] In optimizations, both atomic positions and lattice constants were relaxed, until the forces were smaller than 0.05 eV/Å per atom. Plane-wave energies were bonded by a 450 eV cutoff. The Brillouin zone was sampled with a (5 × 5 x 1) Monkhorst−Pack k-point grid. A more accurate (25 × 25 × 1) grid was used for the projected density of states (PDOS). A vacuum distance of ∼15 Å was set between monolayers to avoid interlayer interactions. We tested the influence of increasing the vacuum distance between monolayers up to ∼20 Å and found it has no impact on the results, suggesting that 15 Å is enough of a distance to avoid the interaction between layers. The six-layer fcc (100) slabs of Co, Ni, and Ag were built from the experimental bulk lattice parameters. Phonon calculations were carried out on a 2 × 2 supercell containing 24 atoms, with PBEsol,[41] using the Phonopy software.[42] Born−Oppenheimer molecular dynamics simulations, BO-MD, were performed using PBE[38] and ultrasoft pseudopotentials, as implemented in Quantum Espresso.[43] Simulations were carried out at 300 K and every 200 K within the range 800−1800 K, controlled via velocity rescaling. The time step was set to 1 fs and the simulations were as long as 8 ps. The chemical bonding analysis was done using the solid state adaptive natural density partitioning (SSAdNDP)[44] tool, which achieves a seamless description of systems featuring both localized and delocalized bonding. Within SSAdNDP, the plane-wave density was projected into the def2-SVP localized atomic orbital basis set.[45]

III. RESULTS AND DISCUSSION

We computationally characterized M_2X monolayers (M = Co, Ni, and X = C, N). After the monolayers were lifted off of the metal surfaces and optimization, the p4g reconstruction and planarity of M_2X persisted (Figure 1, Table 1). The carbides and nitrides are composed of XM_4 squares, where X is located at the center of the metallic void, and M_4 rhombuses. The computed phonon spectra of these p4g phases, with no imaginary modes in the entire Brillouin zone, confirm their kinetic stability (Figure S1). Co_2N, Ni_2N, and Ni_2C materials are completely planar and feature a ptC or ptN. Co_2C is slightly buckled, with the shift of 0.14 Å above and below the plane (Figure 1). The Co_2C monolayer with enforced planarity has three imaginary modes (Figure S2). It is observed that the less electron-rich systems (Co over Ni, carbides over nitrides) are more strongly reconstructed, in agreement with the previous description of surface alloys.[34] Differences in bond lengths are in line with the radii of the constituting elements.
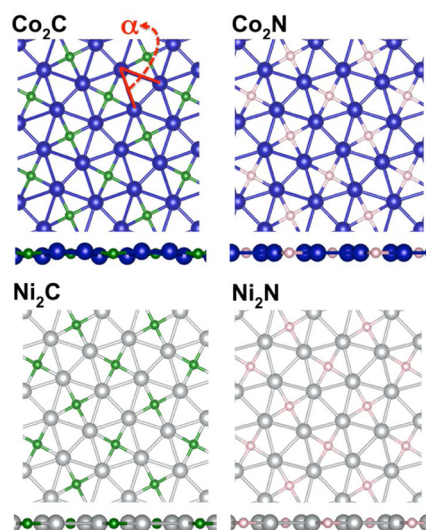

Figure 1. Co_2C, Co_2N, Ni_2C, and Ni_2N monolayers: (top) top view; (bottom) lateral view.

To evaluate the energetic stability of these structures, we calculated the cohesive energy per atom:

$$E_{coh} = (E_{UnitCell} - 2E_X - 4E_M)/6$$

where E_X is the energy of a C or N atom, E_M is the energy of a Co or Ni atom, and $E_{UnitCell}$ is the energy of one unit cell used in calculations. E_{coh} (Table 1) are between ca. −4.2 and −5.0 eV. Despite the absence of interactions in the z-direction, the monolayers compete in stability with the bulk Co and Ni fcc, calculated to be −5.40 and −4.65 eV per atom, respectively. Furthermore, the binding energies of the gas phase C/N to the most stable M(111) monolayers, BE(X), are −4.7 to −9.7 eV. Overall, the stability of the monolayers is very high, and it is the highest for the most electron poor Co_2C.

The binding energies of the monolayers to the parent metallic fcc slab (BE*, Table 1) are rather large too, indicating that the monolayers could be hard to obtain through exfoliation of the parent slabs. However, we find that on (100) fcc silver (whose lattice constant of 4.09 Å is larger than that for Co, 3.35 Å, and Ni, 3.52 Å), the binding energies (BE**) are very small. Thus, we hypothesize that 2D carbides and nitrides could be prepared on, and peeled from, a silver slab. Note that on Ag the monolayers adopt the unreconstructed structure (Supporting Information, Figure S3). This fact will be the subject of our future studies.

To further probe the thermal stability of the proposed 2D alloys, ab initio molecular dynamics (MD) simulations at different temperatures were performed, for Ni_2N as a selected case. We stress that Ni_2N is actually the least stable, judging by energies in Table 1. After 8 ps, the structure remained p4g up to a striking T of 1800 K. During the simulations, the monolayer buckles, with Δz being proportional to T (300 K, 0.3 Å; 800 K, 0.8 Å; 1000 K, 0.9 Å; 1200 K, 1.1 Å; 1400 K, 1.2 Å; 1600 K, 1.2 Å; 1800 K, 1.2 Å). For comparison, snapshots taken at the end of the MD at 300 K and 1800 K can be found in the Supporting Information (Figure S4). Overall, the system exhibits robust thermal stability and at least strong kinetic trapping.

Even though the system never exits the p4g phase in high-T MD, we further checked for its possible reorganization, for the Co_2C case. First, we performed MD simulations at 800 K, with

Table 1. Geometric, Energetic, and Electronic Properties of the Monolayers[a]

	q_X	$R(X–M)$	$R(M–M)$	E_{coh}	α	BE(X)	BE*	BE**
Co_2C	−1.09	1.82	2.58	−5.03	26.85	−14.93	−9.65	−0.51
Co_2N	−1.22	1.78	2.52	−4.54	28.22	−12.02	−8.82	−0.30
Ni_2C	−1.07	1.81	2.56	−4.75	27.60	−15.50	−5.46	−0.63
Ni_2N	−1.28	1.78	2.52	−4.17	30.72	−12.05	−4.66	−0.46

[a]q_X is the Bader charge of C/N, $R(M–X)$ is the metal−C/N distance (Å), $R(M–M)$ is the M−M distance in M_4X (Å), E_{coh} is the cohesive energy (eV), α is the reconstruction angle (Figure 1), BE(X) is the C(N) binding energy to the monolayer with respect to gas phase C(N) and the (111) metallic monolayer, BE* is the binding energy to the parent metallic fcc slab, and BE** is the binding energy to the Ag fcc slab.

the mass of the metal nucleus artificially reduced, and allowing the lattice vectors to change. This resulted in a more rapid exploration of the configurational space. After ca. 3 ps of dynamics, a new phase emerged, formed by triangles and pentagons (Figure 2A). This phase is buckled ($\Delta z > 1$ Å), while
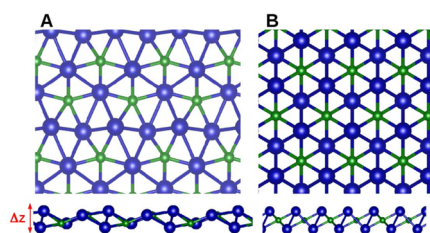

Figure 2. Top and lateral views of the probed (A) "pentagonal" and (B) "hexagonal" buckled phases of Co_2C.

the corresponding planar phase has kinetic instability (Figure S5). No other phases were discovered in MD. Another possible structure could be inspired by the recent work of Yang et al. on a graphene-like structure for Ni_2Ge and Ni_2Si 2D materials, where Ge/Si resides in the center of the Ni_6 hexagon.[46] Although our MD simulations never reached this phase, we manually tested it for Co_2C, Co_2N, Ni_2C, and Ni_2N (Figure 2B). The relative energies of the studied phases (Table 2) are

Table 2. Relative Energies (eV) of the 2D Phases Formed by Squares (p4g Reconstructed), Pentagons, and Hexagons for Each Compound[a]

	p4g	pentagonal	hexagonal
Co_2C	1.31 (0.27)	1.15 (1.34)	0.0 (1.72)
Co_2N	0.0		4.08
Ni_2C	0.64	2.10	0.0 (1.82)
Ni_2N	0.0		5.98

[a]For the buckled cases the buckling distance along z directions, Δz, is given in parentheses (Å) (Figure. 2).

indicative of the high preference of nitrides for the p4g reconstructed phase. Carbides are the most stable in the "hexagonal" but highly buckled phase (Figure 2B), with the corresponding planar monolayers being kinetically unstable (Figure S6). The highly buckled "pentagonal" phase of Co_2C is also slightly more stable than p4g. The 2D nature of these buckled phases, however, can be questioned, as they likely tend toward the 3D bulk, and cannot be considered 2D anymore. Our results taken together allow us to infer that the 2D p4g phase prepared on top of a metal slab and exfoliated should be stable even at high T.

What electronic effects govern the structures of the found p4g 2D phases of Co and Ni carbides and nitrides? The bonding between Co/Ni and C/N is ionic, $q(C/N) \sim -1$, as is

the case with all systems where the presence of ptC is governed electronically.[10] We examined the chemical bonding in our systems via the maximal possible localization of the full electron density, using SSAdNDP (Figure 3). We find this method to produce meaningful results only for closed-shell systems, and therefore we focus the analysis on Ni_2N, as a representative case. In total, there are 50 valence electrons. SSAdNDP localizes four d-AO lone pairs on each Ni atom (occupation numbers, ON = 1.98 and 1.63 |e|). The absence of any classical 2 centers−2 electrons (2c−2e) bonds suggests that the rest of the electrons are delocalized over more than 2c. Four 3c−2e bonds with ON = 1.89 |e| are found, and they arise from the mixing of the 2s atomic orbital (AO) of N with d-AOs of the metal. The remaining 10 electrons are delocalized 5c−2e bonds, shared between all the atoms in the Ni_4N square. Three 5c−2e bonds (ON = 1.99−1.97 |e|) are σ-radical, where 2s-, $2p_x$- and $2p_y$-AOs of N are mixed with the d_{xy}-AOs of Ni. With six delocalized electrons populating these states, the system obeys the (4n + 2) Hückel's rule for local σ-aromaticity in the Ni_4N cycle, with n = 1. In addition, there is a completely bonding 5c−2e σ-peripheral state (ON = 1.97 |e|), arising from the $d_{x^2-y^2}$-AOs of the metal with an insignificant participation of AOs on N. Two electrons in this state make the system additionally σ-peripherally aromatic, with n = 0. Note that the difference between σ-radical and peripheral is the orientation of the atomic orbitals: they point inward in the cycle, i.e., radially, in the σ-radical states, and along the periphery of the cycle in σ-peripheral states. A single π-state (ON = 1.68 |e|) formed by the p_z-AO on N and d_{xz}-AOs on Ni makes the system locally π-aromatic, with n = 0. Overall, the system is 3-fold aromatic: σ-radical, σ-peripheral, and π-radical. This strong stabilizing effect of aromaticity explains the marked preference for the p4g 2D structure. For Ni_2C we found the same bonding pattern (Figure S7). For all alloys, the C/N-binding states lay deep below the Fermi level, E_F, as can be seen in Figure 4. From our previous work,[34] we infer that they are identical for all considered 2D carbides and nitrides, and all of them are stabilized by triple aromaticity. In the work by Yang et al.[46] the SSAdNDP for the buckled phase showed a different bonding pattern from the 2D phase, but also buckling was significant, and accompanied by a large change in charge distribution. This is not the case with our slightly buckled Co_2C. The buckling seems to drive the structure toward somewhat higher compactness, for the enhancement of the bonding overlap (Table 1). In fact, among the considered materials, Co_2C needs to accommodate the elements of the largest relative sizes (atomic radii: C 0.67 Å vs N 0.56 Å; Co 1.52 Å vs Ni 1.49 Å).

The states at E_F remain delocalized. Essentially, some of the d-states of the metal get consumed by the binding of the main group element, but other d-states remain delocalized as in the parent metallic monolayer. In accord with these modest changes in the wave functions, the structures of the monolayers
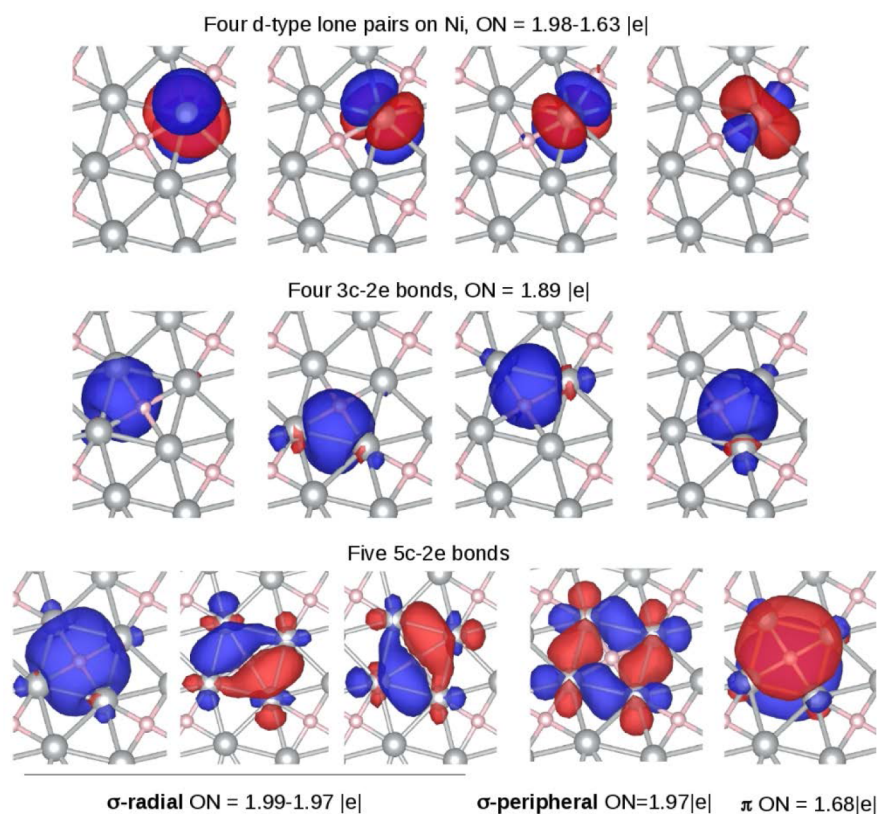
Figure 3. Localized representation of bonding of the Ni₂N monolayer.
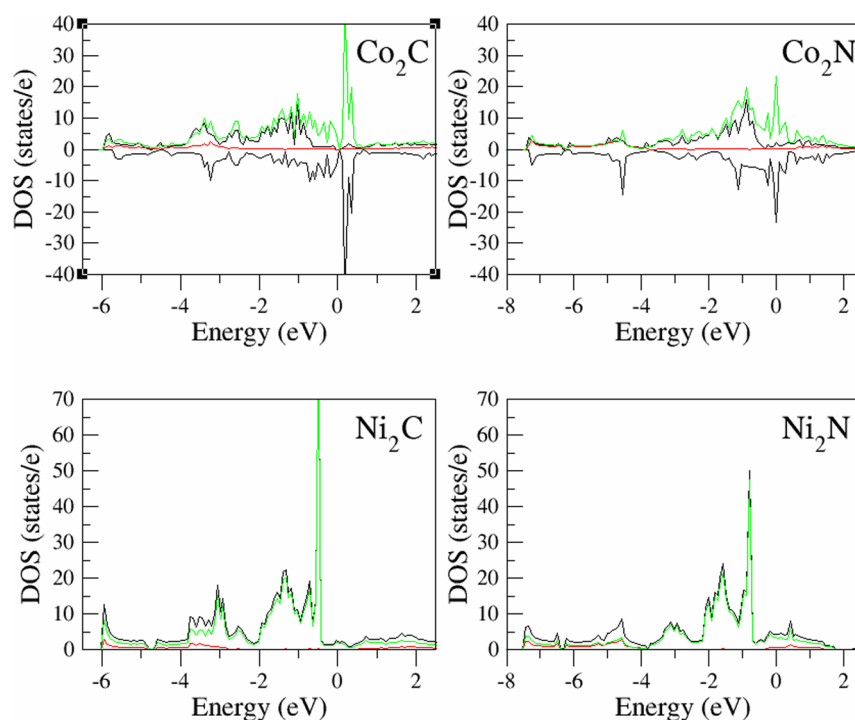

Figure 4. PDOS of the four studied carbides and nitrides, demonstrating their metallic character and, in the case of Co alloys, magnetism: (black) total DOS; (red) DOS of C(N); (green) DOS of Co(Ni).

are perturbed minimally. DFT suggests that all carbides and nitrides are metallic. This can be seen from the projected density of states (PDOS) plots (Figure 4). This result was confirmed using the Hubbard U correction (Supporting Information). It is even more exciting that Co₂C and Co₂N have magnetic properties. We characterized the antiferromagnetic, ferromagnetic, and nonmagnetic states of cobalt compounds, and the relative energies are summarized in

Table 3. Relative Energies (eV) of Ferromagnetic (FM), Antiferromagnetic (AFM), and Nonmagnetic (NM) States of p4g Reconstructed Co_2C and Co_2N

	FM	AFM	NM
Co_2C	0.0	0.19	0.76
Co_2N	0.0	0.002	0.27

Table 3. Although for Co_2C the ferromagnetic state is clearly favored (with a magnetic moment of the unit cell being 4.0 μB), for Co_2N the ferromagnetic (with a magnetic moment 2.6 μB) and antiferromagnetic states are degenerated. The spin density in all cases was found to be largely localized on the metal atoms.

To the best of our knowledge, magnetism is exceedingly rare among stable 2D materials. Applications, for example, in memory devices can therefore be envisioned. Of another notice is the p_z-AO on ptC/ptN: it is involved in the delocalized π-state but essentially remains occupied but uncoordinated. This may indicate its reactivity, affinity for small molecules with accessible vacant MOs for dative bonding, or interesting electronic properties (to-be-discovered in the future).

IV. CONCLUSIONS

To summarize, we propose a new class of metallic, and in some cases magnetic, 2D materials: carbides and nitrides of Co and Ni. These phases feature ptC and ptN coordination, rare in extended systems. 2D phases are predicted to be stable at elevated temperatures. The structure and stability are governed by 3-fold local aromaticity of the M_4X (M = Co, Ni, X = C, N) unit that binds the main group elements. The possible method of preparation of these materials could involve exfoliation off of a slab with a larger lattice constant metal, such as Ag.

ASSOCIATED CONTENT

Supporting Information

The Supporting Information is available free of charge on the ACS Publications website at DOI: 10.1021/acs.jpcc.6b07612.

> Phonon spectra of all studied materials, structures of the monolayers supported on the parent slabs and on the surface of Ag, snapshots from MD trajectory takes at different temperatures, structures and phonon spectra of the planar p4g, "pentagonal", and "hexagonal" Co_2C monolayer, SSAdNDP results for Ni_2C, and calculated DOS with and without Hubbard U (PDF)

AUTHOR INFORMATION

Corresponding Author

*A. N. Alexandrova. E-mail: ana@chem.ucla.edu. Tel: +1 (310) 825-3769.

Notes

The authors declare no competing financial interest.

ACKNOWLEDGMENTS

REFERENCES

(1) Hoffmann, R.; Alder, R. W.; Wilcox, C. F. Planar tetracoordinate carbon. *J. Am. Chem. Soc.* **1970**, 92, 4992−4993.

(2) Siebert, W.; Gunale, A. Compounds containing a planar-tetracoordinate carbon atom as analogues of planar methane. *Chem. Soc. Rev.* **1999**, 28, 367−371.

(3) Erker, G. Using bent metallocenes for stabilizing unusual coordination geometries at carbon. *Chem. Soc. Rev.* **1999**, 28, 307−314.

(4) Collins, J. B.; Dill, J. D.; Jemmis, E. D.; Apeloig, Y.; Schleyer, P. v. R.; Seeger, R.; Pople, J. A. Stabilization of planar tetracoordinate carbon. *J. Am. Chem. Soc.* **1976**, 98, 5419−5427.

(5) Erker, G.; Röttger, D. The energetic stabilization caused by a planar-tetracoordinate carbon atom: A dynamic NMR spectroscopic study of the dimetallabicycle $[(Cp_2Zr)_2(\mu\text{-C-CCH3})(\mu\text{-}H_3CCCCH_3)]BPh_4$. *Angew. Chem., Int. Ed. Engl.* **1993**, 32, 1623−1625.

(6) Radom, L.; Rasmussen, D. R. The planar carbon story. *Pure Appl. Chem.* **1998**, 70, 1977−1984.

(7) Sorger, K.; Schleyer, P. v. R. Planar and inherently non-tetrahedral tetracoordinate carbon: a status report. *J. Mol. Struct.: THEOCHEM* **1995**, 338, 317−346.

(8) Merino, G.; Mendez-Rojas, M. A.; Vela, A.; Heine, T. Recent advances in planar tetracoordinate carbon chemistry. *J. Comput. Chem.* **2007**, 28, 362−372.

(9) Schleyer, P. v. R.; Boldyrev, A. I. A new, general strategy for achieving planar tetracoordinate geometries for carbon and other second row periodic elements. *J. Chem. Soc., Chem. Commun.* **1991**, 1536−1538.

(10) Alexandrova, A. N.; Nayhouse, M. J.; Huynh, M. T.; Kuo, J. L.; Melkonian, A. V.; Chavez, G.; De, J.; Hernando, N. M.; Kowal, M. D.; Liu, C.-P. Selected $AB_4^{(2-/-)}$ (A = C, Si, Ge; B = Al, Ga, In) ions: a battle between covalency and aromaticity, and prediction of square planar Si in $SiIn_4^{(2-/-)}$. *Phys. Chem. Chem. Phys.* **2012**, 14, 14815−14821.

(11) Gribanova, N. T.; Minyaev, R. M.; Minkin, V. I. Planar tetracoordinated nitrogen in boron-containing compounds: a theoretical quantum-chemical study. *Mendeleev Commun.* **2002**, 12, 170−172.

(12) Zhang, W.-Q.; Sun, J.-M.; Zhao, G.-F.; Zhi, L.-L. The structural and electronic properties of $In_nN(n = 1−13)$ clusters. *J. Chem. Phys.* **2008**, 129, 064310.

(13) Averkiev, B. B.; Boldyrev, A. I.; Li, X.; Wang, L.-S. Planar nitrogen-doped aluminum clusters Al_xN^- (x = 3−5). *J. Chem. Phys.* **2006**, 125, 124305.

(14) Cui, Z.; Ding, Y. $NXAl_3^+$ (X = N, P, As): penta-atomic planar tetracoordinate nitrogen with N−X multiple bonding. *Phys. Chem. Chem. Phys.* **2011**, 13, 5960−5966.

(15) Zhang, Z.; Liu, X.; Yakobson, B. I.; Guo, W. Two-dimensional tetragonal TiC monolayer sheet and nanoribbons. *J. Am. Chem. Soc.* **2012**, 134, 19326−19329.

(16) Dai, J.; Wu, X.; Yang, J.; Zeng, X. C. AlxC Monolayer Sheets: Two-dimensional networks with planar tetracoordinate carbon and potential applications as donor materials in solar cell. *J. Phys. Chem. Lett.* **2014**, 5, 2058−2065.

(17) Wu, X.; Pei, Y.; Zeng, X. C. B_2C graphene, nanotubes, and nanoribbons. *Nano Lett.* **2009**, 9, 1577−1582.

(18) Dai, J.; Li, Z.; Yang, J.; Hou, J. A first-principles prediction of two-dimensional superconductivity in pristine B_2C single layers. *Nanoscale* **2012**, 4, 3032−3035.

(19) Zhang, S.; Zhou, J.; Wang, Q.; Chen, X.; Kawazoe, Y.; Jena, P. Penta-graphene: A new carbon allotrope. *Proc. Natl. Acad. Sci. U. S. A.* **2015**, 112, 2372−2377.

(20) Li, F.; Tu, K.; Zhang, H.; Chen, Z. Flexible structural and electronic properties of a pentagonal B_2C monolayer via external strain: a computational investigation. *Phys. Chem. Chem. Phys.* **2015**, 17, 24151−24156.

(21) Pancharatna, P. D.; Mendez-Rojas, M. A.; Merino, G.; Vela, A.; Hoffmann, R. Planar tetracoordinate Ccarbon in extended systems. *J. Am. Chem. Soc.* **2004**, *126*, 15309−15315.

(22) Wang, Y.; Li, Y.; Li, Z. Chem. Semi-metallic Be_5C_2 monolayer global minimum with quasi-planar pentacoordinate carbons and negative Poisson's ratio. *Nat. Commun.* **2016**, *7*, 11488−11502.

(23) Xiao, B.; Yu, X.; Hu, H.; Ding, Y. Beryllium decorated armchair boron nitride nanoribbon: A new planar tetracoordinate nitride containing system with enhanced conductivity. *Chem. Phys. Lett.* **2014**, *608*, 277−283.

(24) Xiao, B.; Cheng, J.; Liu, Z.; Li, Q.; Li, W.; Yang, X.; Yu, X. Beryllium decorated armchair BC_2N nanoribbons: coexistence of planar tetracoordinate carbon and nitrogen moieties. *RSC Adv.* **2015**, *5*, 73945−73950.

(25) Ciobîcă, I. M.; van Santen, R. A.; van Berge, P. J.; van de Loosdrecht, J. Adsorbate induced reconstruction of cobalt surfaces. *Surf. Sci.* **2008**, *602*, 17−27.

(26) Tan, K. F.; Xu, J.; Chang, J.; Borgna, A.; Saeys, M. Carbon deposition on Co catalysts during Fischer−Tropsch synthesis: A computational and experimental study. *J. Catal.* **2010**, *274*, 121−129.

(27) Trinh, Q. T.; Tan, K. F.; Borgna, A.; Saeys, M. Evaluating the structure of catalysts using core-level binding energies calculated from first principles. *J. Phys. Chem. C* **2013**, *117*, 1684−1691.

(28) Banerjee, A.; van Bavel, A. P.; Kuipers, H. P. C. E.; Saeys, M. Origin of the formation of nanoislands on cobalt Ccatalysts during Fischer−Tropsch synthesis. *ACS Catal.* **2015**, *5*, 4756−4760.

(29) Weststrate, C. J.; Kizilkaya, A. C.; Rossen, E. T. R.; Verhoeven, M. W. G. M.; Ciobîcă, I. M.; Saib, A. M.; Niemantsverdriet, J. W. Atomic and polymeric carbon on Co(0001): Surface reconstruction, graphene formation, and catalyst poisoning. *J. Phys. Chem. C* **2012**, *116*, 11575−11583.

(30) Onuferko, J. H.; Woodruff, D. P.; Holland, B. W. Leed structure analysis of the Ni{100} $(2 \times 2)C$ (p4g) structure; A case of adsorbate-induced substrate distortion. *Surf. Sci.* **1979**, *87*, 357−374.

(31) Rieder, K. H.; Wilsch, H. Helium diffraction from Ni(100): A study of the clean surface and of hydrogen and carbon adsorption phases. *Surf. Sci.* **1983**, *131*, 245−257.

(32) Klink, C.; Stensgaard, I.; Besenbacher, F.; Lægsgaard, E. An STM study of carbon-induced structures on Ni(111): evidence for a carbidic-phase clock reconstruction. *Surf. Sci.* **1995**, *342*, 250−260.

(33) Vang, R. T.; Honkala, K.; Dahl, S.; Vestergaard, E. K.; Schnadt, J.; Lægsgaard, E.; Claussen, B. S.; Norskov, J. K.; Besenbacher, F. Ethylene dissociation on flat and stepped Ni(1 1 1): A combined STM and DFT study. *Surf. Sci.* **2006**, *600*, 66−77.

(34) Nandula, A.; Trinh, Q. T.; Saeys, M.; Alexandrova, A. N. Origin of extraordinary stability of square-planar carbon atoms in surface carbides of cobalt and nickel. *Angew. Chem., Int. Ed.* **2015**, *54*, 5312−5316.

(35) Kresse, G.; Hafner, J. Ab initio molecular dynamics for liquid metals. *Phys. Rev. B: Condens. Matter Mater. Phys.* **1993**, *47*, 558. Kresse, G.; Hafner, J. Ab initio molecular-dynamics simulation of the liquid-metal−amorphous-semiconductor transition in germanium. *Phys. Rev. B: Condens. Matter Mater. Phys.* **1994**, *49*, 14251−14269.

(36) Kresse, G. Furthmaller, Efficiency of ab-initio total energy calculations for metals and semiconductors using a plane-wave basis set. *Comput. Mater. Sci.* **1996**, *6*, 15−50.

(37) Kresse, G.; Furthmüller, J. Efficient iterative schemes for ab initio total-energy calculations using a plane-wave basis set. *Phys. Rev. B: Condens. Matter Mater. Phys.* **1996**, *54*, 11169−11186.

(38) Perdew, J. P.; Burke, K.; Ernzerhof, M. Generalized gradient approximation made simple. *Phys. Rev. Lett.* **1996**, *77*, 3865−3868.

(39) Perdew, J. P.; Burke, K.; Ernzerhof, M. Erratum for generalized gradient approximation made simple. *Phys. Rev. Lett.* **1997**, *78*, 1396.

(40) Grimme, S. Semiempirical GGA-type density functional constructed with a long-range dispersion correction. *J. Comput. Chem.* **2006**, *27*, 1787−1799.

(41) Perdew, J. P.; Ruzsinszky, A.; Csonka, G. I.; Vydrov, O. A.; Scuseria, G. E.; Constantin, L. A.; Zhou, X.; Burke, K. Restoring the density-gradient expansion for exchange in solids and surfaces. *Phys. Rev. Lett.* **2008**, *100*, 136406.

(42) Togo, A.; Tanaka, I. First principles phonon calculations in materials science. *Scr. Mater.* **2015**, *108*, 1−5.

(43) Gianozzi, P.; Baroni, S.; Bonini, M.; Calandra, M.; Car, R.; Cavazzoni, C.; Ceresoli, D.; Chiarotti, G. L.; Cococcioni, M.; Dabo, I.; et al. QUANTUM ESPRESSO: a modular and open-source software project for quantum simulations of materials. *J. Phys.: Condens. Matter* **2009**, *21*, 395502−395521.

(44) Galeev, T. R.; Dunnington, B. D.; Schmidt, J. R.; Boldyrev, A. I. Solid state adaptive natural density partitioning: a tool for deciphering multi-center bonding in periodic systems. *Phys. Chem. Chem. Phys.* **2013**, *15*, 5022−5029.

(45) Weigend, F.; Ahlrichs, R. Balanced basis sets of split valence, triple zeta valence and quadruple zeta valence quality for H to Rn: Design and assessment of accuracy. *Phys. Chem. Chem. Phys.* **2005**, *7*, 3297−3305.

(46) Yang, L.-M.; Popov, I. A.; Frauenheim, T.; Boldyrev, A. I.; Heine, T.; Bačić, V.; Ganz, E. Glitter in a 2D monolayer. *Phys. Chem. Chem. Phys.* **2015**, *17*, 26043−26048.

F